Pre- and Post- Processing in Data Assimilation

F. Rabier

CNRM-GAME, Météo-France and CNRS
Toulouse, France
florence.rabier@meteo.fr

1.   Introduction

This paper provides an overview of the details of the data assimilation system implementation, at both pre and post-processing levels, which are, more often than not, mentioned in passing in data assimilation talks or articles. Data assimilation is the art of combining model and observations. It relies on a set of equations grounded on sound statistics. Some theoretical studies investigate ways to define optimally various quantities (observation operators, observation and background error covariances) and how to combine all the flow-dependent information (time evolution of the model, using linearized models in 4D-Var or ensembles in EnKF).

But more is needed to get a reliable and optimal analysis. In practice, a lot of attention has to be paid to details in the handling of observations and about the use of a possible filtering of the resulting analysis. This paper will focus on the details of the implementation, which is also an area of intense research. The various topics covered by this paper are divided as follow: the transformation of the raw data: transforming into a different space, averaging the data and filtering the observations will be described in section 2. The third section will introduce applications of the comparison of data and model or other observations for monitoring and choices of observations, bias correction, and means of removing wrong data. The fourth section will be devoted to the thinning of data, in order to reduce data quantity and error correlation, while choosing the most relevant local data. The last section will deal with the post-processing step, namely the filtering of the analysis, with an introduction to initialisation methods and a presentation of their influence on the analysis.

2.   Transforming data

First of all it is necessary to process raw data, i.e. to transform them so as to get observations that can be easily integrated into a data assimilation system. Amongst the different kinds of observations, radiosondes take simple measurements of such atmospheric parameters as wind, temperature, pressure and humidity. Other observations are very indirect measurements. For example, satellite operators process several series of images from satellites to derive atmospheric motion vectors, tracking a target in an image at consecutive times. Radiances, widely used in Numerical Weather Prediction (NWP), measure the electromagnetic spectrum, and provide very indirect information on temperature, humidity, surface, clouds, ozone and other constituents. These radiances can be used directly in data assimilation schemes, including a radiative transfer model in the observation operator (see Derber's article in the same volume), or via retrievals, where the transformation to atmospheric parameters is performed individually for each vertical profile before the analysis. Some NWP centres combine these

two approaches, starting with a one-dimensional retrieval of some parameters at the observation points, also useful for quality control, followed by the assimilation of radiances in a full 3D or 4D-Var scheme using some of the retrieved parameters such as surface temperature, emissivity or cloud parameters as input.

The second step of data pre-processing consists of spatial averaging. Some of the horizontal averaging can be performed by data producers as is the case for the Clear Sky Radiances, averaged in boxes typically of 16*16 pixels for SEVIRI on board MSG at EUMETSAT. Some averaging can also be done at user's level. In the pre-processing of all-sky radiances at ECMWF, it was found that averaging observations to create AMSR-E super-observations at a 80km scale was beneficial (Geer and Bauer, 2010). Another example is the processing of satellite winds at the Naval Research Laboratory (NRL). NRL produces super-observations with a complex algorithm, averaging in boxes (prisms of about 2-degree side, then performing prism-quartering when there is a high degree of variability within the box, and checking that observations agree within a certain range (Pauley, 2003). Their processing of satellite winds is more elaborate than at other NWP centres and they are found to get more positive results from these data than at other centres (Gelaro et al, 2010).

At meso-scale, a similar averaging is performed for radar data. Radar winds are pre-processed in a similar fashion in the HIRLAM 3D-Var (Lindskog et al, 2004) and at NCAR for WRF (Zhang et al, 2009). Super-observations are created from radial winds by averaging in polar space. These super-observation winds are smoother than the raw data and representative on spatial scales characteristic for the averaging procedure (Figure 1). To avoid averaging radial winds with significant different directions, fewer polar bins are used near the radar than at longer ranges. At Météo-France, a median concept is used rather than a mean value (Montmerle and Faccani, 2009). A median filter is applied on boxes of 5*5 pixels, replacing observed values by the median of neighbouring points.
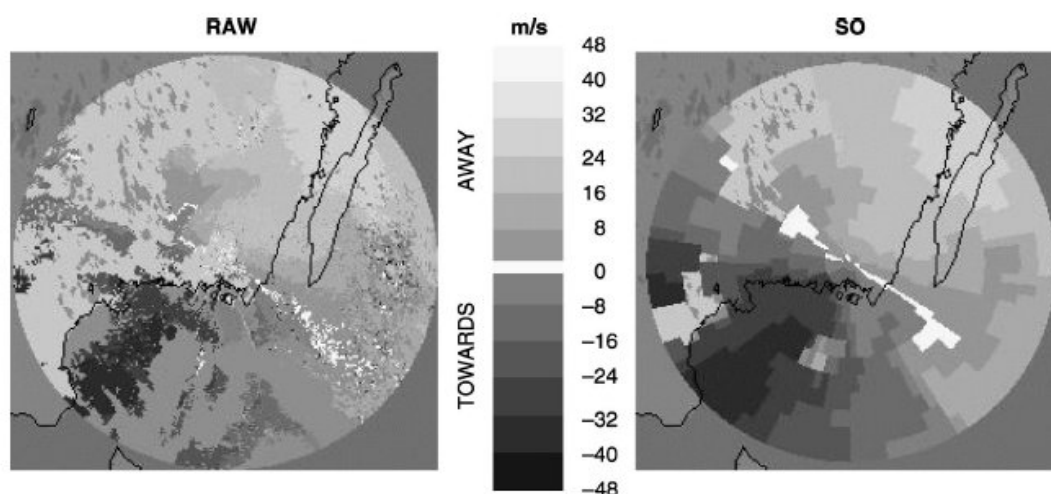

Figure 1: Averaging of radial winds from raw data (left) into super-observations (right). From Lindskog et al, 2004.

Averaging data can also be performed in the time dimension. For example, the GPS ground-based system provides integrated water vapour at high temporal frequencies. In Europe, depending on the operators, GPS observation time periods can range from 5 to 60 minutes. For these data, a time-averaging of observations is performed, with a 30 to 60 minute period compatible with the length of the 4D-Var slots (Poli et al, 2007; McPherson et al, 2008). Similarly, time-averaging can be performed for NCEP Stage IV radar and gauge precipitation data, used at ECMWF for example. Hourly data can be used, but 6-hourly accumulations are found to perform better. Thus, the correlation between departures computed in the full trajectory (T799 resolution with full physics) and in first minimisation (T95, with simplified physics) increases from 0.2 to 0.7. This can be seen as a compromise between linearity and observation usage over the 4D-Var 12-hour window (Lopez, 2011).

Finally, the treatment of the observations in the vertical will be discussed. A vertical choice of data is performed for some observations: typically one might select only one observation per model level (this is usually the case for aircraft or radio-occultation observations). For radiosonde observations, the transmission of data to NWP centres follows some rules: observations are transmitted either if they are on mandatory levels (fixed pressure levels) or if they are at a significant level in the vertical profile corresponding to a change in slope. As these observations are the backbone of the global observing system, all levels are usually kept in the assimilation. At meso-scale, one might even interpolate between significant and mandatory levels to yield additional data points (Benjamin et al, 2004). This forces the analysis to fit the near-linear structures implied by the absence of intermediate significant levels. In the future, more data points will be transmitted and the processing might change, possibly forcing centres to average data in the vertical, or to select only a subset of points.

Processing of hyper-spectral sounder data provides new challenges. At each pixel, thousands of radiances describe the infra-red part of the spectrum. Each channel is sensitive to various quantities (mainly temperature or humidity), and to a certain vertical slice of the atmosphere. One needs to compress the information contained in the hyperspectral sounder data to make their assimilation possible. The idea then is to select the most relevant channels to describe adequately all parameters of interest. For instance, such a channel selection was studied for the Atmospheric Infra Red Sounder AIRS and for the Infrared Atmospheric Sounding Interferometer IASI (Fourrié and Thépaut, 2003; Rabier et al, 2002; Collard, 2007) and an approach based on the information content was found to be particularly effective. The channel that most improves the Degrees of Freedom for Signal DFS is selected, where DFS is the Trace of the matrix $I-AB^{-1}$, with B the background error covariance matrix and A the analysis error covariance matrix after using this channel. Once this most informative channel is chosen, the A matrix is updated and the next best channel chosen and so forth. This process is applied to a set of representative atmospheric profiles in order to produce an optimal set of channels, valid in most conditions. These are the channels which are going to be assimilated in NWP (Figure 2).

Principal component compression is also envisaged (Collard et al, 2010). Principal components are computed from a large set of spectra, and principal component amplitudes can then be related to observed radiances. It is found that around 200 principal components are required to represent the signal, the rest being considered as noise. Using the leading principal components is then efficient for data transfer and noise filtering. It is a well suited method to represent the relatively small amount of information contained in spectra. But, as pointed out by Collard et al (2010), this new way of handling data means that we will have to adapt the way we deal with these observations. In particular, there are
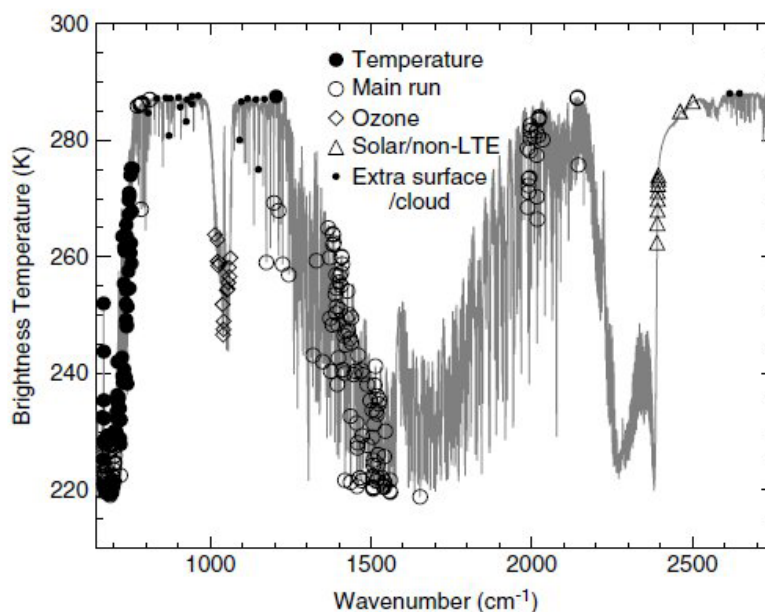
Figure 2: Channel selection (300 channels) for the IASI hyperspectral sounder, illustrated on an observed spectrum. From Collard, 2007.

still pending issues, such as the introduction of error correlations, extending the current practice of selecting channels not affected by surface/cloud, and monitoring (identifying faulty channels that are sensitive to given levels in the atmosphere).

3.   Comparing data and models

The comparison of the observations to the model and the choice of the relevant data to be used, usually make up the second part of the post-processing step. This process is called the monitoring of observations. Examples at NWP centres show that changes in the vertical or horizontal resolution of the model can, for instance, allow the model to fit more closely high-peaking channels or ground-based synoptic stations. These might then be considered for assimilation, as they can now be "represented" by the model. Some choices have to be made, not only about which channel or which synoptic station to select, but also about the amount of precipitation threshold in a dataset for example. At the Japanese Meteorological Agency (JMA), the radar rain-gauge data are assimilated at fine-scale in 4D-Var with a simplified cloud microphysics scheme. Honda and Yamada (2007), showed that the initial choice of using radar data only when the observed 1-hour rain was greater than 0.5mm did not allow the analysis to remove spurious precipitation. This was achieved by changing the threshold to 0mm.

The presence of bias is another issue to be dealt with. The monitoring procedure usually shows the presence of systematic differences between model and observations, and part of this bias seen in the monitoring can be attributed to observations. Simple to elaborate bias correction schemes have been devised. On the simple side, ground-based GPS data are usually treated with a bias correction simply based on averaged deviations from the model (Poli et al, 2007), or on a 10-day running mean

(McPherson et al, 2008). For other types of observations, such as radiosondes, the physical processes originating the bias, which depends on a few factors, such as sonde type, sonde age, solar elevation, pressure level are known beforehand. If one can identify a more precise, almost bias-free sonde type, one can then deduce the bias from the other sonde types by comparison. This is what was done by Nuret et al (2008) during the AMMA field campaign over Africa. For a limited time period in 2006, a scattered sampling was achieved at Niamey (Niger) for Vaisala RS-80A and RS-92 sonde types, using 4 sondes of each type, every day, for 25 days. As RS-92 is the newest, more precise type of radiosonde, it served as basis for the RS-80 one. Agusti-Panareda et al (2009) went a step further, still considering that the RS-92 was almost bias-free (at least at night) and using the model as an intermediate thus assuming that the model biases have the same characteristics everywhere. A Cumulative Distribution Function matching is performed, followed by a fitting of four-sine wave components of a Fourier series depending on the observed humidity, for each pressure level, solar elevation, and sonde type (Figure 3). The monitoring biases are computed both for the reference sonde Oref (Vaisala RS-92) and for any sonde O. Then, the bias of the sonde O is written as Bias (O-Oref)= Bias (O-B)-Bias(Oref-B), where B is the model background (short-range forecast). As both biases were computed beforehand, the bias for sonde O can now be computed.

For satellite radiances, an a priori knowledge about the parameters affecting the observation bias is known. Harris and Kelly (2001) used scan-dependence and air-mass predictors to describe the bias, with regression coefficients computed over a long time-series. The selected air-mass predictors are the model thicknesses (1000-300hPa, 200-50hPa,…), the surface temperature and the integrated water content. The regression coefficients can be adapted off-line before any analysis, or inside the assimilation (the so-called Variational bias-correction, Auligné et al, 2007, further mentioned in the article by Derber in the same volume).

Comparing model and observations is also useful in removing erroneous data. Each observation is subject to a variety of errors: biases from calibration, random errors, representativeness errors but also gross errors coming from instrument malfunction or transmission error for instance. Data with gross errors are useless and need to be eliminated by a quality control step.

Removing data with a history of frequent gross errors is done through a so-called "blacklist" which identifies all suspect observations generally based on monthly monitoring. The blacklist can also be dynamically updated, based on gross-error statistics from a few previous analyses (De Pondeca et al, 2011).

In real-time, to spot these errors, one also checks that observations are consistent and that all values are within reasonable physical limits. « Buddy checks » is another powerful tool, whereby one checks that an observation is consistent with its neighbours (Benjamin et al, 2004). An estimate of the innovation at the observation point is obtained from the innovations of a group of nearby observations by Optimal Interpolation. If the difference between the estimated and observed innovations exceeds a threshold, the observation is discarded. This procedure generally uses a flow-dependent background error structure, and therefore is quite adaptive.
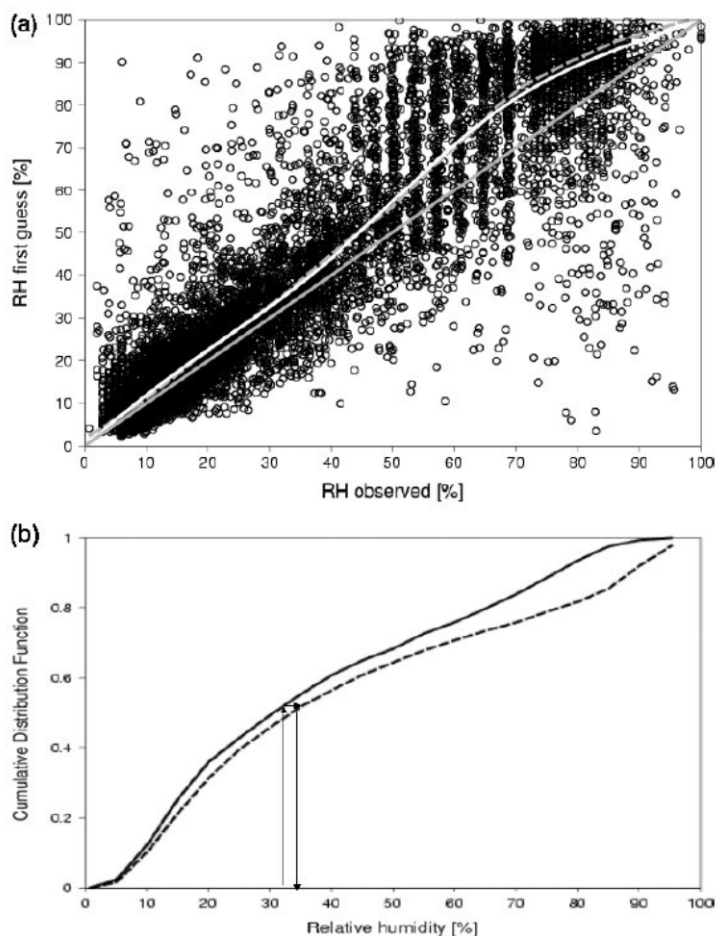
Figure 3: Scatter plot of first guess versus observed relative humidity for Vaisala Digicora I, II radiosondes at 925 hPa and positive soar elevation larger than 27,5°. The grey solid line is the density line. The grey dashed curve shows the bias obtained from CDF matching the white solid curve is the best fit using four sine waves. (b) Cumulative distribution function for observation (solid line) and first guess (dashed line). Arrows illustrate the CDF matching techniqiue described in the text. From Agusti-Panarela et al. 2009.

Finally, the so-called « First-guess check » is commonly applied to models. Check tests are based on the comparison of departures with error estimates, observation error variances (De Pondeca et al, 2011), background error variances (Benjamin et al, 2004), or more generally, a combination of both (Lorenc and Hammon, 1988; Cucurull et al, 2007). Assuming that both observations and background have Gaussian distribution, then the difference (the innovation, or departure) will also have a Gaussian distribution, with a sum of variances as the total variance. When the squared departure gets too large compared to this resulting variance multiplied by a certain factor, one can assume that the observation is wrong.

More often than not, an interactive combination of such tests is performed, with interactions between them. For example, different norms can be used (ex : Huber norm at ECMWF) to represent departure statistics inside the assimilation and adapt the prior First-Guess check accordingly. In Dee et al (2001), the authors explain how their adaptive buddy check, using flow-dependent tolerances for outlier observations is combined with the First-Guess check. Observations which are flagged by the First-Guess check are subject to a buddy check. Only non-suspect observations are used in the prediction

step of the buddy check. If some suspect observations pass the check, then the partitioning is updated accordingly and the buddy check is repeated. This leads to an iterative procedure that ends when no additional data pass the test. The remaining suspect data are rejected. But, if accepted by buddy check, they enter the analysis. The implied tolerance in the buddy-check scheme is locally adjusted for each buddy check, and recomputed at each iteration, based on the observed variability of nearby data that have already passed the quality control. In relatively data-dense areas, this results in decisions that are not very sensitive to prescribed statistics. Figure 4 illustrates the performance of the scheme in the December 1999 storm case over France. The adaptive algorithm is able to adjust the tolerance for the iterative buddy check scheme and bring in the majority of observations, resulting in an improved analysis (at 18UTC, the actual low is 969hPa, and the analysis of surface pressure goes down from 979 to 974 hPa when going from the non-adaptive to the adaptive scheme).

Finally, it should be mentioned that one can now use more reliable flow-dependent "errors of the day" in these a-priori checks, thanks to the new application of Ensemble Data Assimilation at various centres (eg Berre and Desroziers, 2010; Bonavita et al, 2011).
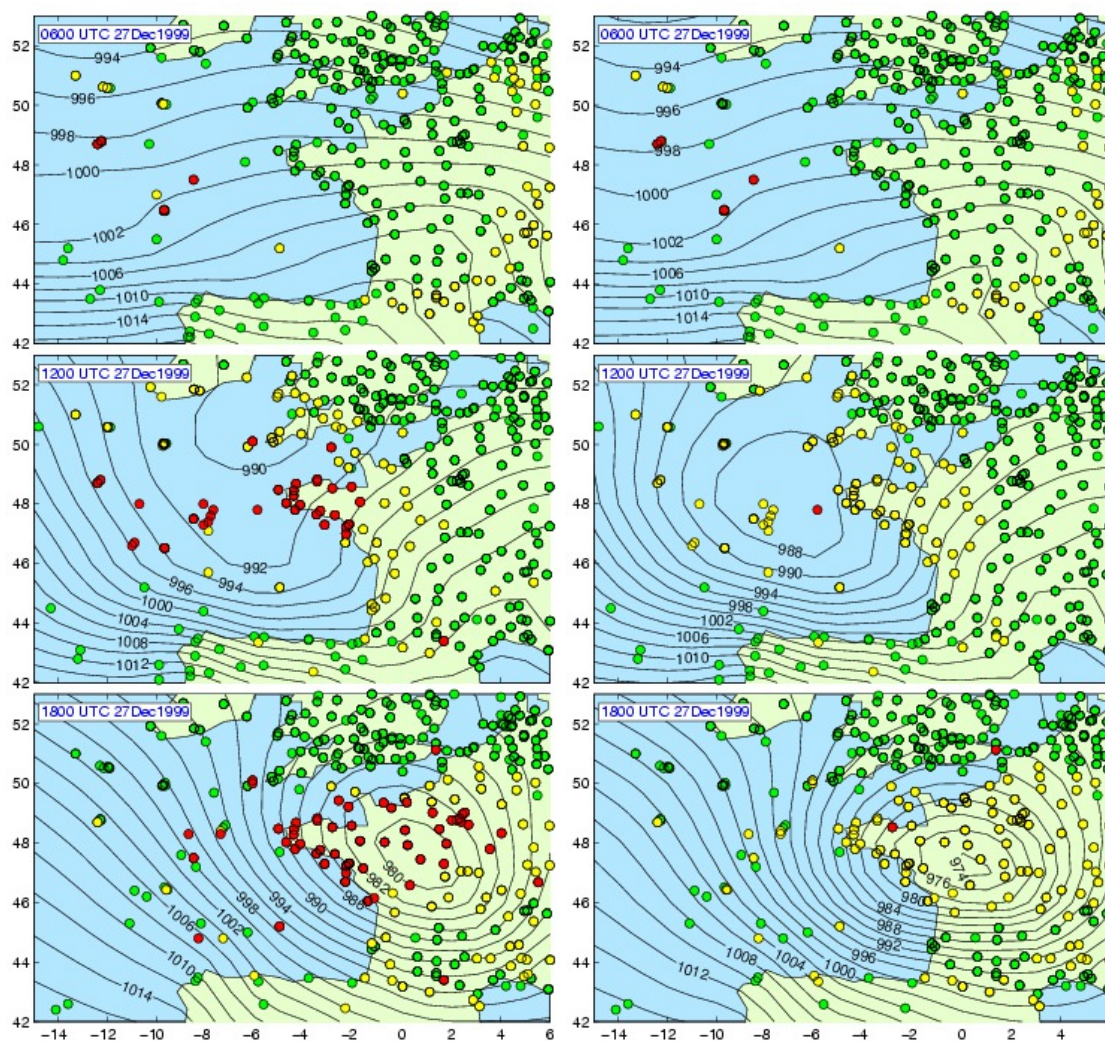

Figure 4: Observations passing the First-Guess check (green), failing the First-Guess check by passing the Buddy check (yellow), and failing both (red), in a non-adaptive setting (left-hand side) and an adaptive scheme (right-hand side). From Dee et al (2001).

4. Thinning the dataset

Different analysis schemes use different temporal thinning of data. In 4D-Var, one groups observations in 30 or 60 minute time-slots and thin observations within each time-slot. In a 3D-Var, one usually selects data closer to the central analysis time (ex: +/- 1.5 hour for aircraft data). In non-cycled schemes, data are chosen to be really representative of analysis time. For example, for the hourly Real-time Mesoscale Analysis (De Pondeca et al, 2011), the time window is selected so as to be within +/–12 minutes of the analysis time.

For dense datasets such as those provided by satellite sounding data, a horizontal thinning is performed, both for practical cost reasons, and to avoid observation error correlations between adjacent observations, which are not accounted for in assimilation schemes. Generally, the thinning is performed in a simple manner, by latitude-longitude boxes. Within each box, the observation is selected according to a given quality criterion, for example: distance to guess, Quality Indicator provided by the data producer, small value of radial wind variance in the super-observation, maximum number of elevations which pass the quality control in radar profiles. More elaborate adaptive thinning techniques have been devised by Ochotta et al (2005) where either observations representative of clusters are inserted iteratively, or, observations from the full set are removed if they are considered redundant.
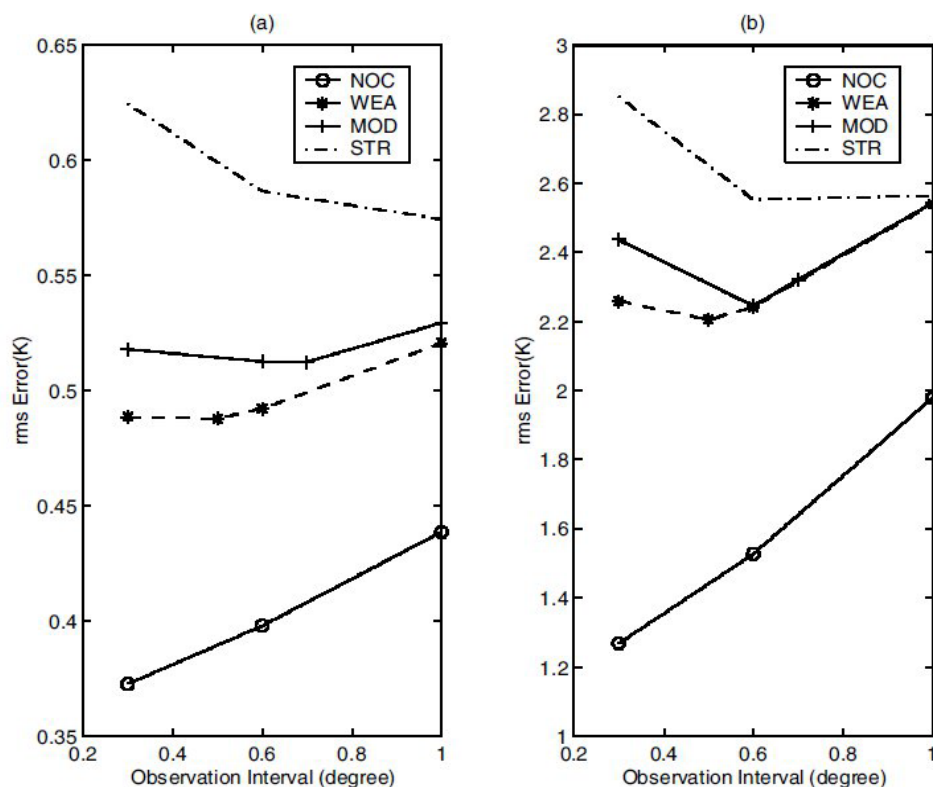

Figure 5: RMS of analysis and 48-hour forecast errors as a function of observation interval in the context of simulated AMSU-A radiances, for which the observation error correlation is zero (solid lines with circles), weak (dashed lines with stars), moderate (solid lines with crosses) and strong (dash-dotted lines). From Liu and Rabier, 2003.

In a simulated observation context, Liu and Rabier (2002 and 2003) showed that, for uncorrelated errors, using more observations always improves the analysis, but this does not hold for correlated errors. To neglect the observation error correlation can indeed deteriorate both the analysis and the forecast if it becomes too large. Depending on the strength of the observation correlation, an "optimal" thinning distance was found to preserve a reasonable quality in the analysis. An example is shown in Fig.5.

In fact, such correlations exist in meteorological satellite observations, as demonstrated for atmospheric motion vectors by Bormann et al (2003), and for satellite radiances by Bormannn and Bauer (2010), Bormann et al (2010), which justify the practice of thinning in NWP centres.

In a real-observations context, the optimal thinning distance was investigated in the Met Office NWP system by Dando et al (2007) over a three-week period.
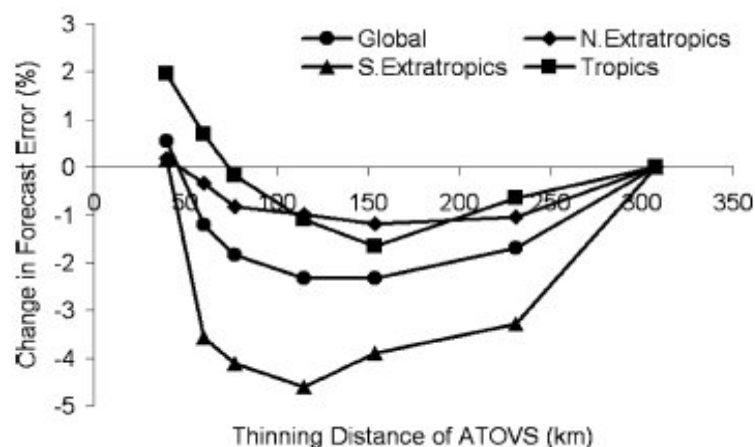

Figure 6: Change in forecast error based on different ATOVS thinning distances in the analysis, for different regions, compared to a reference (308km thinning). From Dando et al (2007).

The control experiment used a thinning distance of 308km for ATOVS data. Then, this distance was altered for other experiments, and the quality of the resulting analysis was judged by the quality of the associated forecasts. An optimal distance was found to be between 100 and 150km. In particular, it was found detrimental to use thinning at the finest 40-km distance, especially in Tropics where weak gradients are present in the meteorological fields. The reason put forward is that at high densities, the outcome may be determined by the meteorological features associated with the most influential analysis errors. If the analysis errors responsible for the majority of the forecast error are in a region of strong gradient, additional ATOVS observations may be beneficial. With active weather systems in the extra-tropics, the highest densities may have a positive impact on the analysis.

This reasoning was used in another context at ECMWF, in which optimal AMSU-A thinning using Singular vector information was performed in the Southern Hemisphere (Bauer et al, 2011). Several configurations were tested over two seasons: an experiment with a global density of 1.25°, an experiment with a global High-density of 0.625°, an experiment with High-density only in areas determined by the singular vectors of the day (Buizza et al, 2000), an experiment with High-density

only in areas determined by the climatological singular vectors, and an experiment with High-density in random areas. Firstly, it was shown that the High density experiment always performed better than any others. It was further demonstrated that in the warm season, singular-vector-based thinning performs significantly better than random or climatological thinning. Finally, the global density enhancement is found to be very positive at high latitudes and locally negative in the Tropics. Singular-vector-based thinning initially produced a smaller impact that gradually amplifies to a consistent positive impact. In winter, results were more mixed, probably due to the fact that more data are rejected in cloudy areas and over sea-ice lessening differences between scenarios.

In the Ensemble Kalman Filter context, the radius of influence of observations (ROI) also plays a role in the quality of the analysis. An example is given by Zhang et al (2009). In WRF, radar wind data assimilation is performed in 3 domains D1 (40km) to D3 (4.5km) over the US in a case of tropical cyclone with a 30-member EKF. Several experiments are performed with either fixed ROIs in each domain, from 1215km to 135km. Other experiments are performed with ROI varying from 1215km to 135km from the largest domain D1 to the smallest domain D3. The best experiment uses a successive covariance localization, with a different localization radius of influence used for different groups of observations by random sampling. First, one tries to dynamically remove important aspects of the large-scale errors by assimilating a relatively small subset of observations with a large radius of influence. Next, this radius is decreased and higher-density observations are used to constrain both smaller-scale errors and remaining large-scale errors. This approach is motivated by the fact that with the EnKF performing serial observation processing, the error correlation length scale decreases since large scales are better defined by the previously assimilated observations.

5.   Filtering the analysis

During the forecast, the model can take time to adjust initial fields with respect to the model equations. This « spin-up » contains processes of dynamical adjustment with excess energy radiated away by inertia-gravity waves, and processes of diabatic adjustment where model physics tendencies converge with respect to other model forcings. Ideally, the analysis should create balanced increments through the background-error covariance matrix. There is also a possibility to include constraint terms inside the analysis (Gauthier and Thépaut, 2001). But in practice, it is still often necessary to perform a posterior filtering of the analysis. With this procedure, the initial state cannot generate model tendencies that project onto high-frequencies model solutions, using some filtering, removing spurious waves which can affect the first hours in the forecast and thus the assimilation cycle. Amongst the different methods that can be used, the two most popular ones are the Digital Filter Initialization (DFI, Lynch and Huang, 1992; Huang and Lynch, 1993) and the Incremental Analysis Update (IAU, Lorenc et al, 1991; Bloom et al, 1996). DFI implies running the model backward and forward and then filtering the high frequencies choosing a cut-off frequency. In the forward step, the model can be run in diabatic mode, with the physical tendencies. IAU consists in spreading the insertion of the increment in a time window around the nominal analysis time, with direct insertion over a few timesteps. Initial imbalance, as measured by the time tendency of the surface pressure over the domain of interest for example, depends on the quality of the analysis. Chen and Huang (2006), showed that, the Cressman analysis points to more imbalance in the initial fields than the 3D-Var analysis (Figure 7). Similarly, in the Rapid Update Cycle, Benjamin et al (2004) found less balance in fields initialized with Optimum Interpolation than with a 3D-Var. Similarly, in the Rapid Update Cycle, Benjamin et al (2004) have found less balance in fields initialized with Optimum Interpolation than with a 3D-Var.

Initialization can quite drastically change the resulting initial condition fields. One way to counteract this major impact is to perform incremental initialization (Fischer and Auger, 2011).

Let us denote $X_a^* = DFI(X_a)$ the filtered analysis state after standard DFI.

The increment for standard DFI is then $X_a^* - X_b = DFI(X_a) - X_b = \{DFI(X_a) - DFI(X_b)\} + \{DFI(X_b) - X_b\}$.

It is the sum of a balanced increment and of the result of an operation removing the high frequencies in x_b. In the Incremental DFI, the filtered state is $X_a^* = X_b + \{DFI(X_a) - DFI(X_b)\}$, and the total increment is then $X_a^* - X_b = DFI(X_a) - DFI(X_b)$.

If one admits the existence of high frequencies in the background that are not filtered by DFI in relation to rapidly developing meteorological features for example, it is better not to filter them out, and to privilege the incremental approach.
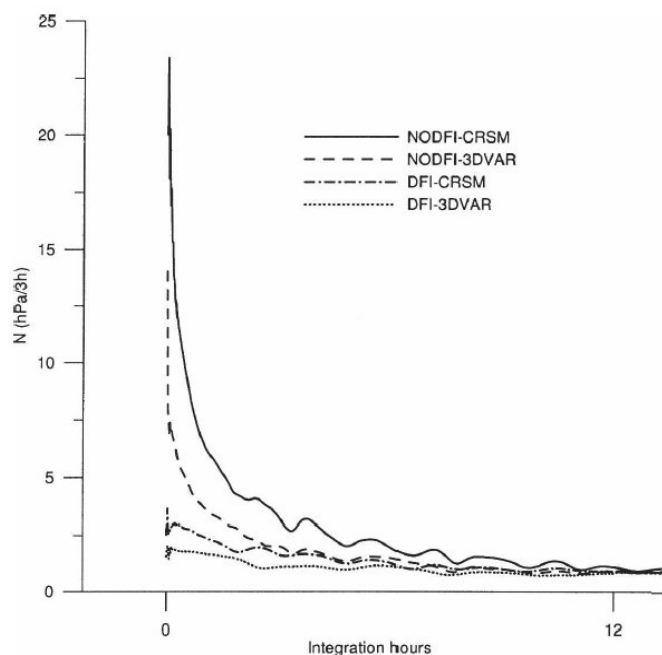

Figure 7: Imbalance measures from different initial conditions, before and after the application of DFI. The analyses are performed with a Cressman or an OI method. This figure shows the evolution of the mean absolute surface pressure tendency N [hPa(3h)$^{-1}$ in the first 12-h forecast averaged from 14 cycles from 0000 UTC 21 Aug to 1200 UTC 27 Aug 2002. From Chen and Huang (2006)

Filtering is effective not only for forecasts, but also for the assimilation. For rapid cycles, the assimilation cycle can be adversely affected by spurious waves which have to be filtered out before the next cycle is performed, so as to compare the model fields with new observations from a noise-free forecast. This is becoming more important as the tendency is to go to hourly cycles for fine-scale data assimilation.

6.   Conclusions

As has been illustrated above, in a NWP real-world context, there is much more to data assimilation than solving a mathematical equation with an optimality criterion. A whole area of research is devoted to more practical issues such as the processing of observations or the filtering of the analysis. This is justified by the fact that a single erroneous observation can destroy the structure of an important meteorological feature such as a tropical cyclone, and that noise in the forecast can make it impossible for the forecasters to use it in the first forecast ranges. Therefore, the importance of these issues should not be under-estimated.

References

Agustí-Panareda, A., Vasiljevic, D., Beljaars, A., Bock, O., Guichard, F., Nuret, M., Garcia Mendez, A., Andersson, E., Bechtold, P., Fink, A., Hersbach, H., Lafore, J.-P., Ngamini, J.-B., Parker, D. J., Redelsperger, J.-L. and Tompkins, A. M., 2009: Radiosonde humidity bias correction over the West African region for the special AMMA reanalysis at ECMWF. *Q.J. Roy. Meteorol. Soc.*, **135**: 595–617. doi: 10.1002/qj.396

Auligné, T., McNally, A. P. and Dee, D. P., 2007: Adaptive bias correction for satellite data in a numerical weather prediction system. *Q.J. Roy. Meteorol. Soc.*, **133**: 631–642. doi: 10.1002/qj.56

Bauer, P., Buizza, R., Cardinali, C. and Noël Thépaut, J., 2011: Impact of singular-vector-based satellite data thinning on NWP. *Q.J. Roy. Meteorol. Soc.*, **137**: 286–302. doi: 10.1002/qj.733

Benjamin S. G., D. Devenyi, S. S. Weigandt, K. J. Brundage, J. M. Brown, G. A. Grell, D. Kim, B. E. Schwartz, T. G. Smirnova, and T. L. Smith, 2004: An Hourly Assimilation-Forecast Cycle: The RUC. *Mon. Wea. Rev.*, **132**, 495-518

Berre, L. and G. Desroziers, 2010: Filtering of background error variances and correlations by local spatial averaging: A review. *Mon. Wea. Rev.*, **138**, 3693–3720. doi: 10.1175/2010MWR3111.1

Bloom S.C., L.L. Takacs, A.M. Da Silva, and D. Ledvina, 1996: Data Assimilation Using Incremental Analysis Updates. *Mon. Wea. Rev.*, **124**, 1256-1271.

Bonavita M., L. Raynaud, L. Isaksen, 2011: Estimating background-error variances with the ECMWF Ensemble of Data Assimilations system: some effects of ensemble size and day-to-day variability. *Q.J. Roy. Meteorol. Soc.*, **137**, 423-434. DOI: 10.1002/qj.756

Bormann N; Saarinen S; Kelly G; and J-N. Thépaut, 2003: The spatial structure of observation errors in atmospheric motion vectors from geostationary satellite data. *Mon. Wea. Rev.*, **131**, 706-718

Bormann N. and P. Bauer, 2010: Estimates of spatial and interchannel observation-error characteristics for current sounder radiances for numerical weather prediction. I: Methods and application to ATOVS data. *Q.J. Roy. Meteorol. Soc.*, **136**, 1036-1050   DOI: 10.1002/qj.616

Bormann N., A. Collard and P. Bauer, 2010: Estimates of spatial and interchannel observation-error characteristics for current sounder radiances for numerical weather prediction. II: Application to AIRS and IASI data. *Q.J. Roy. Meteorol. Soc.*, **136**, 1051-1063   DOI: 10.1002/qj.615

Buizza, R., J. Barkmeijer, T.N. Palmer and D.S. Richardson, 2000: Current status and future developments of the ECMWF Ensemble Prediction System. *Meteor. Applic.*, **7**, 163-175 DOI: 10.1017/S1350482700001456

Chen, M. and X. Y. Huang, 2006: Digital Filter Initialization for MM5, *Mon. Wea. Rev.*, **134**, 1222-1236

Collard, A.D, 2007: Selection of IASI channels for use in numerical weather prediction. *Q.J. Roy. Meteorol. Soc.*, **133**, 1977-1991 DOI: 10.1002/qj.178

Collard, A.D., A.P. McNally, F.I. Hilton, S.B. Healy and N.C. Atkinson, 2010: The use of principal component analysis for the assimilation of high-resolution infrared sounder observations for numerical weather prediction. *Q.J. Roy. Meteorol. Soc.*, **136**, 2038-2050 DOI: 10.1002/qj.701

Cucurull, L., J.C., J.C. Derber, R. Treadon and R. J. Purser, 2007: Assimilation of global positioning system radio occultation observations into NCEP's global data assimilation system. *Mon. Wea. Rev.*, **135**, 3174-3193 DOI: 10.1175/MWR3461.1

Dando, M.L., A.J. Thorpe and J.R. Eyre, 2007: The optimal density of atmospheric sounder observations in the Met Office NWP system. *Q.J. Roy. Meteorol. Soc.*, **133**, 1933-1943 DOI: 10.1002/qj.175

Dee, D.P., L. Rukhovets, R. Todling, A.M. Da Silva, J.W. Larson, 2001: An adaptive buddy check for observational quality control *Q.J. Roy. Meteorol. Soc.*, **127**, 2451-2471 DOI: 10.1256/smsqj.57713

De Pondeca1, M.S.F.V , G. S. Manikin, G. DiMego, S.G. Benjamin, D.F. Parrish, R.J. Purser, W-S Wu, J.D. Horel, D.T. Myrick, Y. Lin, R.M. Aune, D. Keyser, B. Colman, G. Mann, and J. Vavra, 2011: The Real-Time Mesoscale Analysis at NOAA's National Centers for Environmental Prediction: Current Status and Development. *Weather and Forecasting*, accepted.

Fischer C. and L. Auger, 2011: Some Experimental Lessons on Digital Filtering in the ALADIN-France 3DVAR Based on Near-Ground Examination, *Mon. Wea. Rev.*, **139**, 774-785 DOI: 10.1175/2010MWR3388.1

Fourrié N. and J-N. Thépaut, 2003: Evaluation of the AIRS near-real-time channel selection for application to numerical weather prediction. *Q.J. Roy. Meteorol. Soc.*, **129**, 2425-2439 DOI: 10.1256/qj.02.210

Gauthier P. and J-N. Thépaut, 2001: Impact of the digital filter as a weak constraint in the preoperational 4DVAR assimilation system of Météo-France. *Mon. Wea. Rev.*, **129**, 2089-2102.

Geer A.J and P. Bauer, 2010: Enhanced use of all-sky microwave observations sensitive to water vapour, cloud and precipitation. ECMWF Technical Memorandum N° 620.

Gelaro, R, R.H. Langland, S. Pellerin, R. Todling, 2010: The THORPEX Observation Impact Intercomparison Experiment. *Mon. Wea. Rev.* **138**, 4009-4025. DOI: 10.1175/2010MWR3393.1

Harris, B.A. and G. Kelly, 2001: A satellite radiance-bias correction scheme for data assimilation. *Q.J. Roy. Meteorol. Soc.*, **127**, 453-1468   DOI: 10.1256/smsqj.57417

Honda, Y. and Y. Yamada, 2007: Assimilation of the Surface Precipitation Data with JnoVA using 2-ice Bulk Microphysics Scheme. *SOLA*, **3**, 073-076, doi:10.2151/sola.2007-019

Huang X.-Y and P. Lynch, 1993: Diabatic Digital-Filtering Initialization: Application to the HIRLAM model. *Mon. Wea. Rev.*, **121**, 589-603

Lindskog, M., K. Salonen, H. Jarvinen, D.B. Michelson, 2004: Doppler radar wind data assimilation with HIRLAM 3DVAR. *Mon. Wea. Rev.*, **132**, 1081-1092
DOI: 10.1175/1520-0493(2004)132<1081:DRWDAW>2.0.CO;2

Liu, Z.Q. and F. Rabier, 2002: The interaction between model resolution, observation resolution and observation density in data assimilation: A one-dimensional study. *Q.J. Roy. Meteorol. Soc.*, **128**, 1367-1386   DOI: 10.1256/003590002320373337

Liu, Z.Q. and F. Rabier, 2003: The potential of high-density observations for numerical weather prediction: A study with simulated observations. *Q.J. Roy. Meteorol. Soc.*, **129**, 3013-3035
DOI: 10.1256/003590003769682156

Lopez, P., 2011: Direct 4D-Var Assimilation of NCEP Stage IV Radar and Gauge Precipitation Data at ECMWF. *Mon. Wea. Rev.*, **139**. 2098-2116   DOI: 10.1175/2010MWR3565.1

Lorenc, A.C. and O. Hammon, 1988: Objective quality-control of observations using Bayesian methods – Theory, and a practical implementation. *Q.J. Roy. Meteorol. Soc.*, **114**, 515-543 DOI: 10.1002/qj.49711448012

Lorenc, A.C., R.S. Bell and B. McPherson, 1991: The Meteorological-Office analysis correction data assimilation scheme *Q.J. Roy. Meteorol. Soc*., **117**, 59-89   DOI: 10.1002/qj.49711749704

Lynch, P. and X.-Y. Huang, 1992: Initialization of the HIRLAM model using a digital filter. *Mon. Wea. Rev.*, **120**, 1019-1034.

Macpherson, S.R.; G. Deblonde and J.M. Aparicio, 2008: Impact of NOAA ground-based GPS observations on the Canadian regional analysis and forecast system. *Mon. Wea. Rev.*, **136**, 2727-2746   DOI: 10.1175/2007MWR2263.1

Montmerle, T. and C. Faccani, 2009: Mesoscale assimilation of radial velocities from Doppler radars in a preoperational framework. *Mon. Wea. Rev.*, **137**, 1939-1953
DOI: 10.1175/2008MWR2725.1

Nuret, M., J.P. Lafore, O. Bock, F. Guichard, A. Agusti-Panareda, J.B. N'Gamini and J.L. Redelsperger, 2008: Correction of humidity bias for Vaisala RS80-A Sondes during the AMMA 2006 Observing Period. *J. Atmos. Ocean. Technol.*, **25**, 2152-2158
DOI: 10.1175/2008JTECHA1103.1

Ochotta, T., C. Gebhardt, D. Saupe, W. Wergen, 2005: Adaptive thinning of atmospheric observations in data assimilation with vector quantization and filtering methods. *Q.J. Roy. Meteorol. Soc.*, **131**, 3427-3437   DOI: 10.1256/qj.05.94

Pauley, P. 2003: Superobbing Satellite winds for NAVDAS. Report from the Naval Research Laboratory. PDF Url : ADA411981

Poli, P., P. Moll, F. Rabier, G. Desroziers, B. Chapnik, L. Berre, S.B. Healy, E. Andersson, F.Z. El Guelai, 2007: Forecast impact studies of zenith total delay data from European near real-time GPS stations in Meteo France 4DVAR. *J. Geophys.Res.Atmospheres*, **112**, - D06114 DOI: 10.1029/2006JD007430Poli et al, 2007

Rabier, F., N. Fourrié, D. Chafai and P. Prunet, 2002: Channel selection methods for Infrared Atmospheric Sounding Interferometer radiances. *Q.J. Roy. Meteorol. Soc.*, **128**, 1011-1027 DOI: 10.1256/0035900021643638

Zhang, F., Y. Weng, J.A. Sippel, A. Meng, C.H. Bishop, 2009: Cloud-resolving hurricane initialization and prediction through assimilation of Doppler radar Observations with an Ensemble Kalman Filter. *Mon. Wea. Rev.*, **137**, 2105–2125. doi: 10.1175/2009MWR2645.1